Mechanism Study on *Betula* Wood Dowel Rotation Welding into Larch and Enhanced Mechanism of Treating with $CuCl_2$

Xudong Zhu,[a,b] Yingying Xue,[a] Jie Shen,[a] Lingling Huang,[a] and Ying Gao [b,*]

Mechanical properties and chemical changes of wood dowel welding were studied using untreated and copper chloride ($CuCl_2$)-treated *Betula* wood dowels. The effects of the welding times (3 s, 5 s, and 7 s) and the highest temperatures in the welding interface were also studied. The treated wood dowels with a welding time of 3 s and the highest temperature of 265.6 °C had the best pullout resistance. Wood constituents were pyrolyzed by the frictional heat generated from rotational welding to form oxygen-containing materials, most of which were C-O materials. With the extension of welding time, welding interface materials were pyrolyzed deeper, but the rate of pyrolysis decreased, which indicated that the pyrolysis of hemicellulose and cellulose might have occurred in the prior period of the welding process. Acid hydrolysis of hemicellulose and cellulose of the wood dowel treated with $CuCl_2$ might have occurred during immersion, which promoted the formation of molten materials by the depolymerization and pyrolysis of wood constituents. With the same welding time, the content of oxygen-containing materials with treated samples was higher than with untreated samples, which might indicate that more pyrolysis and molten reactions occurred in the treated welding interface.

Keywords: Wood dowel welding; Pullout resistance; Highest temperature; $CuCl_2$; Pyrolysis

*Contact information: a: Yangzhou Polytechnic Institute, Jiangsu 225100, China; b: Beijing Key Laboratory of Wood Science and Engineering, Beijing Forestry University, Beijing 100083, China; *Corresponding author: gaoying@bjfu.edu.cn*

INTRODUCTION

Wood dowel welding creates a new bonding interface layer through the friction between the wood dowels and substrate holes. It has been used to enhance the mortise and tenon interference fit connection and fabricate full-scale multi-layered timber beams and wooden load-bearing walls (Bocquet *et al.* 2007; Mougel *et al*. 2011; O'Loinsigh *et al*. 2012; Fukuta *et al*. 2017). Based on the analysis of wood dowel welding, Korte *et al*. (2018) changed the wood dowel essentially into a wood nail to study the structural deformation and lignin modification.

Several researchers have studied the properties influenced by rotational speed, insertion speed, moisture content, welded depth, and pretreatment (Sandberg *et al*. 2013; Zhou *et al*. 2014; Luo *et al*. 2017). With changes in the parameters above, the highest temperature and the temperature distribution of the welding interface were influenced during the welding process. In the research of Zoulalian and Pizzi (2007), the highest temperature of the welding interface reached 183 °C for beech with optimal parameters. Furthermore, the influence of species and rotational speed have been studied. The highest temperatures of birch and maple were more than 300 °C at 2500 rpm (Rodriguez *et al*. 2010). For both birch and maple, the temperature reached 244.1 °C and 282.6 °C at 1000

rpm and 281.1 °C and 297.4 °C at 1500 rpm, respectively. According to the pullout resistance, the samples of birch and maple from the highest temperatures of 244.1 °C and 282.6 °C showed the best properties, respectively (Belleville *et al*. 2013b). In this study, according to the previous experiments, rotational speeds of 1080 rpm, 2400 rpm, and 4000 rpm were studied, as well as the substrate species of larch and spruce. The larch with rotation speed of 2400 rpm showed the highest pullout resistance (Zhang *et al*. 2018).

Under the action of high frictional temperature, pyrolysis occurs at the welding interface. Some wood components are softened, fused, and eventually become solidified until the friction stops. This is considered to be a non-volatilization conversion of materials into volatile mixtures (Sun *et al*. 2010). For a new species used in wood welding, several tests should be conducted to determine the welding properties and chemical changes. Australian eucalypts were a new studying object several years ago. First, mechanical tests were applied to assess the potential of wood welding (Belleville *et al*. 2016, 2017), and then the chemical changes were determined by pyrolysis-gas chromatography/mass spectrometry (PY-GC/MS), X-ray photoelectron spectroscopy (XPS), and thermogravimetric analysis (Belleville *et al*. 2019). According to the highest temperature analysis, the welding interface reached 340 °C during the welding process (Zhang *et al*. 2018). The hemicellulose and lignin were pyrolyzed into molten materials composed of xylans, furans, and flowing lignin (Delmotte *et al*. 2008; Rodriguez *et al*. 2010; Belleville *et al*. 2013a; Amirou *et al.* 2017a). Recrystallized xylans and furanic compounds are generated from the pyrolysis of carbohydrates (Pizzi *et al*. 2006). The smoke generated from the welding process is composed of water vapor, carbon dioxide, and other nontoxic volatile degradation compounds (Omrani *et al*. 2008).

The mechanism of wood dowel welding has been studied by several researchers (Pizzi *et al*. 2006; Stamm *et al*. 2006; Auchet *et al*. 2010; Rodriguez *et al*. 2010). The wood welding enhancement mechanism has also been studied by different pretreatment methods. The physical enhancement methods have been mainly smaller diameters for the substrate holes and dry wood dowel, as well as non-vertical welding (Kanazawa *et al*. 2005). The chemical enhancement methods included wood dowels immersed by ethylene glycol and welding joints pretreated with citric acid, a lignin additive, and wood extractives additive (Pizzi *et al*. 2004, 2011, 2013; Peña *et al.* 2015, 2016; Amirou *et al.* 2017b). In the previous study, the influence of welding time and pretreatment with $CuCl_2$ was studied (Zhu *et al*. 2018). The degree of crystallinity and the pyrolysis changes were determined by X-ray diffraction and thermogravimetric analysis, respectively. In this study, the elements changes and chemical group changes were detected by XPS and PY-GC/MS. Based on these analyses, the mechanism of *Betula* wood dowel welded into *Larch* and the enhancement mechanism of the wood dowel treated with $CuCl_2$ were studied in this paper.

EXPERIMENTAL

Materials

Wood dowels, 10 mm (Chen and Lyu 2018) in diameter and 100 mm in length, were fabricated from birch wood (*Betula pendula*; Suzhou Crownhomes, Suzhou, China). The air-dried density at 12% moisture content (MC) of the birch dowel was 557 kg/m^3. Chinese larch (*Larix gmelinii*; Suzhou Crownhomes, Suzhou, China) slats with the dimensions of 40 mm (tangential, T) × 50 mm (radial, R) × 500 mm (longitudinal, L) were used as substrates. The air-dried density at 12% MC of the larch was 680 kg/m^3.

All the wood dowels were placed in an oven at 63 °C until 2% MC was reached. The tensile strength of the wood dowels was 4864 N. Half of the wood dowels were immersed in 500 mL of 0.1 mol/L $CuCl_2$ solution for 30 min at 20 °C and 60% relative humidity (RH). After immersion, the wood dowels were placed in an oven until the MC was 2% again. The tensile strength of the wood dowels treated with $CuCl_2$ was 4791 N. The decision to use the temperature of 63 °C was based on preliminary experiments. It was found that the wood dowels achieved the desired MC over 2 d at that temperature with minimal warping or cracking. All of the substrates were exposed to a temperature of 20 °C and RH of 60% until reaching a 12% equilibrium MC.

Specimen preparation

The wood substrates were pre-drilled with holes that were 8 mm in diameter and 30 mm (Chen *et al*. 2019) in depth using a drilling machine (Proxxon TBH Type 28 124; Proxxon, Stuttgart, Germany). Next, the wood dowels were welded into the pre-drilled holes in the substrates to create bonded joints at a high-speed rotation. In previous research, the influence of rotational speeds of 1080 rpm and 2400 rpm was studied. For 1080 rpm, almost no smoke was found during the welding process. For 2400 rpm, smoke and black molten material spilled from the interface. According to the pullout resistance test, the pullout resistance of specimens with rotational speed of 2400 rpm was 50.24% higher than that of specimens with rotational speed of 1080 rpm. In contrast, the pullout resistance decreased remarkably when the rotation speed was 4000 rpm (Leban *et al*. 2008). According to the analyses above, a rotational speed of 2400 rpm was selected in this paper. Rotation of the wood dowel stopped when fusion and bonding was achieved after 3 s, 5 s, and 7 s (Belleville *et al*. 2013b). Thirty specimens were prepared for each group, but several specimens were broken during welding or the testing process. Groups A, B, and C were manufactured from the untreated wood dowels (untreated groups). Groups D, E, and F were manufactured from the $CuCl_2$-immersed wood dowels (treated groups).

Methods

Pullout resistance test

After welding, the wood slats were cut into 10 parts that were even in length so that every welded dowel was 40 mm (T) × 50 mm (R) × 50 mm (L) in size. The specimens were conditioned at 20 °C and 60% RH for 7 d before the tests were conducted (Chen *et al*. 2018).

The pullout resistance of the specimens was tested using a universal testing machine (Fig. 1, WDW-300E; Jinan Popwil Instrument Co., Jinan, China) that pulled the welded wood dowels out of the substrate at a speed of 2 mm/min (O'Loinsigh *et al*. 2012). The specimens were fixed by clamping the dowel into the jaw of a fixed beam, while the substrate block was fixed to a mobile beam *via* a metal framework.

Temperature analyses

Six specimens for each group were used for the temperature test. The temperature was tested using six thermocouple sensors with the data collecting device (XSL-A16XS1V0, Beijing Heshi Xingye Technology Co., Ltd., Beijing, China). Six sensors were set in six different depths along 5 mm, 10 mm, 15 mm, 20 mm, 23 mm, and 28 mm (Fig. 2). The response speed of the K-type thermocouple sensor was 0.34 ms.

Fig. 1. WDW-300E universal testing equipment

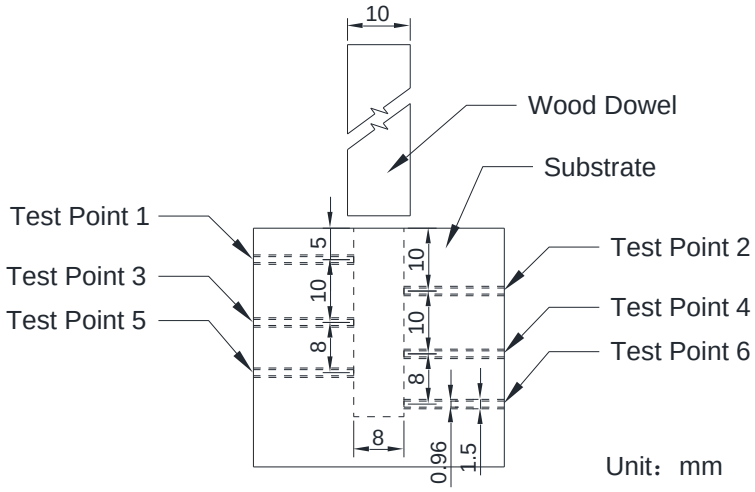

Fig. 2. Temperature test method

Sample preparation for XPS and PY-GC/MS analyses

X-ray photoelectron spectroscopy was used to analyze the surface elements of the wood dowel, the wood dowel treated with $CuCl_2$, and the welding interface for each group. All the powders were prepared from specimens of each group. The sample of wood dowel and welding interface were from the same specimen, and the $CuCl_2$-immersed wood dowel and welding interface similarly were from the same specimen. The surface samples of the untreated and treated wood dowels were cut transversally from the non-welded part of the wood dowels, and the surface samples of the welding interface were cut from the welded part of the wood dowels (Belleville *et al.* 2013a). The XPS analyses were obtained with a spectrometer (ESCALAB 250Xi; Thermo Fisher Scientific, Waltham, MA, USA) and used to provide quantitative data to verify the elementary composition of the same surfaces. The angle of the emitted photoelectrons was 30° to the surface, the source type was Al K Alpha, and the analyzer mode was a pass energy of 100.0 eV with an energy step size of 1.000 eV and a total of 1361 energy steps. The binding energy scale was corrected with reference to the 284.6 eV C-C bond, and a XPSpeak41 software was applied for the curve-fitting of the C1s and O1s spectra.

The samples were pyrolyzed at 550 °C in a helium atmosphere using an EGA/PY-3030D pyrolyzer (Frontier Laboratories, Koriyama, Japan) that was interfaced to a gas chromatograph and a mass spectrometer (QP2010-Ultra; Shimadzu, Kyoto, Japan). The flow rate of the carrier gas was 1.0 mL/min. The pyrolysis interface and GC injector were kept at 250 °C. The pyrolysis was completed from 250 °C (holding for 10 s) to pyrolysis temperature (holding for 30 s) with a heating rate of 6 °C/ms. The GC oven was kept at 45 °C for 4 min and then heated to 280 °C at 4 °C/min. The final temperature was held for 15 min. The mass spectrometer was operated in the electron impact mode using 70 eV energy and the mass range from 40 m/z to 400 m/z was scanned in 36 s. The compounds were identified by comparing the obtained mass spectra with those from Wiley and NIST computer libraries as well as those reported in literature. Relative compound distributions were calculated for each carbohydrate and lignin-derived pyrolysis product from the relevant peak areas.

RESULTS AND DISCUSSION

Pullout Resistance and the Highest Temperature

The pullout resistances of the welded specimens are summarized in Table 1. Group D with the $CuCl_2$-immersed wood dowels and a welding time of 3 s showed the highest pullout resistance. Group C with the untreated wood dowels and a welding time of 7 s showed the lowest pullout resistance. Welding time was an important influencing factor for all groups. For the untreated groups, the pullout resistance of group A was 28% and 87% higher than that of groups B and C, respectively. For treated groups, the pullout resistance of group D was 61% and 130% higher than that of groups E and F, respectively. Considering the treated method of $CuCl_2$-immersed wood dowels, the pullout resistance of the treated groups was 68%, 34%, and 37% higher than that of the untreated groups at the welding times of 3 s, 5 s, and 7 s, respectively.

Table 1. Pullout Resistance of the Welded Specimens for Each Group

Group	Treated with $CuCl_2$	Welding Time (s)	Maximum Value (N)	Minimum Value (N)	Mean Value (N)	COV[2] (%)	Number of Specimens
A	No	3	3602	2072	2790 (444)[1]	15.92	25
B	No	5	3024	1056	2174 (553)	25.45	20
C	No	7	2434	722	1491 (509)	34.15	17
D	Yes	3	6094	3006	4695 (714)	15.21	26
E	Yes	5	3836	1584	2915 (709)	24.34	19
F	Yes	7	2614	1208	2037 (428)	21.01	17

[1]Values in parentheses are the standard deviation; [2]coefficient of variation

Based on the welding phenomenon during the welding process, the highest temperature of the welding interface was observed for each group. From Table 2, for the untreated and treated groups, the highest temperature of the same test point was higher with the extension of welding time. This was caused by the longer time of application of friction in the welding interface, which resulted in more molten material with high heat generated. The relationship between the highest temperature and the welding depth was found. With the larger welding depth, the highest temperature was lower, as the inserted part of the wood dowel became conical in shape with the different abrasion levels during the welding

process. The friction between wood dowel and the pre-drilled hole was decreased along the welding depth.

Based on the research by Zoulalian and Pizzi (2007), the highest temperature 183 °C is the optimal parameter in the welding interface for birch. In the study by Belleville *et al*. (2013a), the highest temperatures with optimal parameters are 244.1 °C and 282.6 °C for sugar maple and yellow birch, respectively. In this study, 344.0 °C and 265.6 °C were the optimal highest temperatures for the untreated and treated groups, respectively, with the birch dowel and larch substrate.

Table 2. The Highest Temperature with Each Point for Untreated and Treated Groups

Group	Highest Temperature (°C)					
	Test Point 1	Test Point 2	Test Point 3	Test Point 4	Test Point 5	Test Point 6
A	344.0	282.9	259.2	182.8	155.6	100.9
B	356.1	295.1	271.1	200.3	173.4	116.2
C	360.7	314.9	279.1	208.3	163.7	113.1
D	265.6	235.8	211.9	203.6	184.2	103.6
E	274.8	246.3	230.1	225.3	200.9	118.5
F	292.0	269.2	252.7	238.3	206.1	111.8

XPS Analysis

Untreated groups

The XPS survey scan spectra of the untreated groups are shown in Fig. 3. The elements C and O were the main components in the wood dowel and welding interface. As the amount of the element C decreased, the element O increased after the welding process. In Table 3, the surface elemental constituents and oxygen/carbon (O/C) ratios of the wood dowel and welding interface were calculated. The amount of C in the wood dowel was higher than that of the welding interface. Meanwhile, the amount of C of the welding interface decreased with extended welding time. In contrast, the amount of O increased because the pyrolysis oxidation reaction of wood components have occurred during the welding process, especially the increase of free phenol and the fracture of an ether bond from the lignin phenylpropane unit.

From Table 3, the O/C ratio of group A was 55% higher than that of the wood dowel, while the O/C ratio of group B was just 16% higher than that of group A. This was caused by the large amount of oxygenated substance generated during the early stage of the welding process. With extended welding time, the time of friction between the wood dowel and substrate hole was prolonged, and more oxygenated substance was generated. However, the increase of oxygenated substance was lower than that of the early stage of welding. According to the phenomena of welding, black molten materials with oxygenated substance spilled out of the welding interface. These black molten materials did not proceed to be oxidized, and the oxidation degree of the new generated black molten materials for group B was similar to that of group A. Therefore, the O/C ratio of group B was slightly higher than that of group A.

Compared with group B, the O/C ratio of group C decreased when the welding time was extended to 7 s. From Table 3, the O/C ratio of group C was lower than that of group B, but higher than that of group A. This phenomenon was caused by two factors. First, it was similar to group B, in that black molten materials spilled out of the welding interface. Second, a large amount of smoke was generated during the welding process. According to

the analyses on the smoke, the main components of the smoke were carbon dioxide and steam, which caused the decrease of elements C and O, and the decrease of O was slightly higher than that of C.

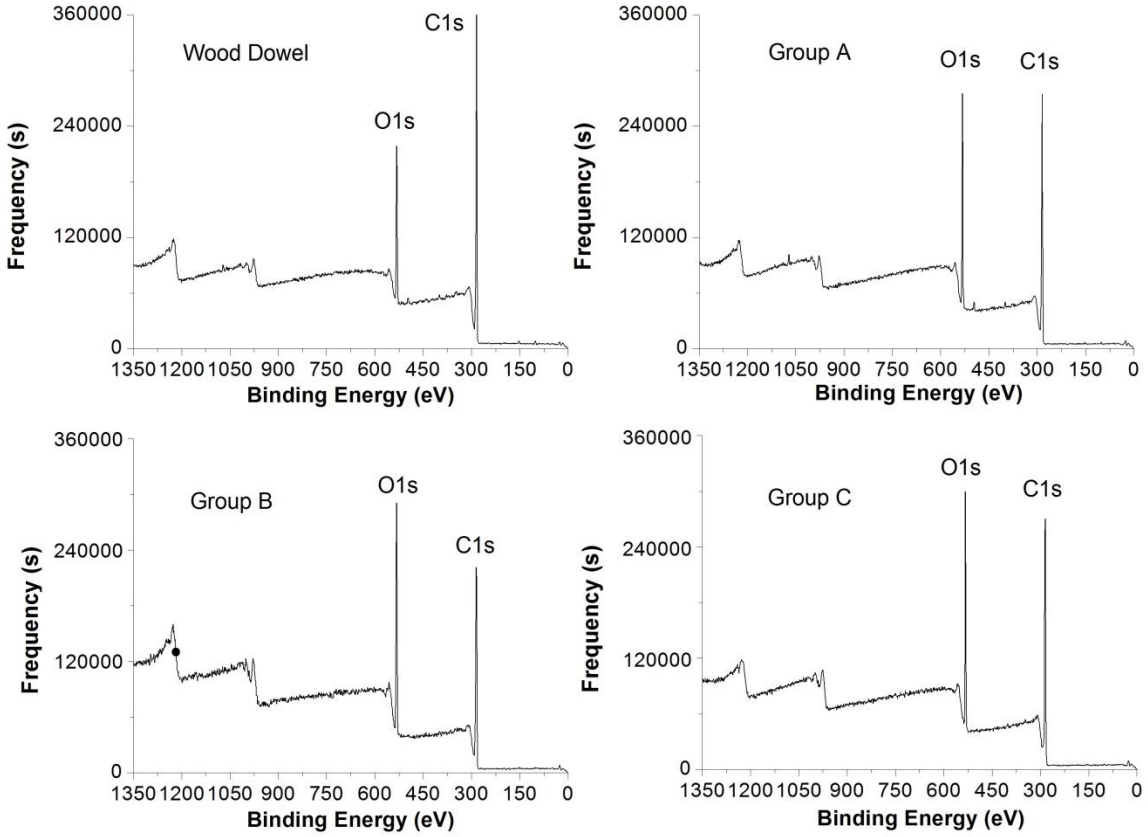

Fig. 3. XPS survey scan spectra of untreated group

Table 3. Surface Elemental Constituent and Oxygen/Carbon Ratio of Wood Dowel and Welding Interface with Each Group

Test Group	Elements (%)					Ratio (%)
	C	O	Cu	Cl	Other	O/C
Untreated wood dowel	82.57	16.27	0	0	1.16	19.70
Group A	75.63	23.10	0	0	1.27	30.54
Group B	73.01	25.91	0	0	1.08	35.49
Group C	74.64	24.56	0	0	0.80	32.90
Treated wood dowel	79.75	18.72	0.11	0.31	1.11	23.47
Group D	74.59	23.37	0.36	0.28	1.39	31.33
Group E	72.14	26.51	0.25	0.19	0.92	36.75
Group F	76.03	22.91	0.13	0.12	0.81	30.13

The quantitative analyses were performed by peak fitting for the C1s and O1s categories. Deconvolution for the three types of carbon bonds and two types of oxygen bonds was performed (Table 4) for the peaks from the wood dowel and welding interface. The three types of carbon bonds were determined as C1 class (C-C/C-H bonds, 284.6 eV), C2 class (C-O bonds, 286.5 eV), and C3 class (C=O/O-C-O bonds, 287.9 eV). The two types of oxygen bonds were determined as O1 class (C=O bonds, 531.8 eV) and O2 class

(C-O bonds, 532.9 eV) (Sun *et al*. 2010). From the analyses of binding energy from 286 eV to 288 eV, the strength of welding interface was noticeably better than that of the wood dowel. It was illustrated by the increase of C2 and C3 with oxygenated substance, which was similar to the analyses of the surface elemental constituent.

Table 4. Results of the Fits of C1s and O1s Region of Wood Dowel and Welding Interface with Each Group

Test Group	C1s (%)			O1s (%)	
	C1	C2	C3	O1	O2
Untreated wood dowel	81.34	12.42	6.24	26.98	73.02
Group A	63.63	28.31	8.06	24.88	75.12
Group B	58.48	32.69	8.83	12.40	87.60
Group C	61.46	31.01	7.53	8.54	91.46
Treated wood dowel	75.52	16.59	7.89	30.44	69.56
Group D	62.30	28.55	9.15	23.03	76.97
Group E	56.19	33.35	10.46	16.61	83.39
Group F	53.08	33.01	13.91	15.11	84.89

From Table 4, it was found that the contents of C2 and C3 in the welding interface were higher than that of the wood dowel, while the content of C1 was lower. This was caused by three aspects. The first contribution was by furan, furfural, and furfural derivative generated from the pyrolysis of amorphous polysaccharides. Secondly, phenol and carbonyl compounds were generated from the depolymerization of lignin. Thirdly, phenolic substances were generated from the –OH thermal oxidation of lignin (Stamm *et al*. 2006). With the extension of welding time, the decrease of C1 was greater, and the relative content of oxygenated substances C2 and C3 increased. This can be attributed to the oxidation of the surface material of the wood dowel and the oxygen-containing groups of alcohol, ether, and phenol generated by the oxidation during the welding process, which resulted in the higher relative increase of C2. The relative content of C2 and C3 of group C was lower than that of group B. This was caused by a large amount of molten materials and smoke that spilled out of the welding interface.

From Table 4, the contents of O1 and O2 in welding interface were identified. The content of O2 for the welding interface was higher than that of the wood dowel, which was illustrated by the increase of the C-O bond in the welding interface. This was the same result as shown by the analyses of C1s. With the extended welding time, the content of O2 still increased. This was caused by the oxygen-containing material generated during the welding interface, especially the C-O group substance.

Based on the above analysis, the mechanism of *Betula* wood dowel welded into *Larch* was that fiber was covered by the molten materials of pyrolyzed hemicellulose and amorphous materials in the welding interface during the rotational friction process. Wood constituents were pyrolyzed by the frictional heat generated from rotational welding to form oxygen-containing materials, most of which were C-O materials. With the extension of welding time, welding interface materials were pyrolyzed deeper, but the rate of pyrolysis decreased, which indicated that the pyrolysis of hemicellulose and cellulose might have occurred in the prior period of the welding process.

Treated groups

The XPS survey scan spectra of the treated groups are shown in Fig. 4. It was found that the tendency of the elements C and O was similar to that of untreated groups. From

Table 3, for the treated groups, the amount of C was the highest. With the extension of welding time, the amount of C decreased while O increased, and the O/C ratio grew. The O/C ratio of group D was 33% higher than that of the treated wood dowel, and the O/C ratio of group E was 17% higher than that of group D. These two phenomena were similar to that of the untreated groups. When the welding time was 7 s, the O/C ratio decreased, which was different from the untreated groups. The O/C ratio of group F was just higher than that of the treated wood dowel, but was lower than that of groups D and E. It was caused by more molten materials and smoke spilling from the welding interface of group F than that of group C.

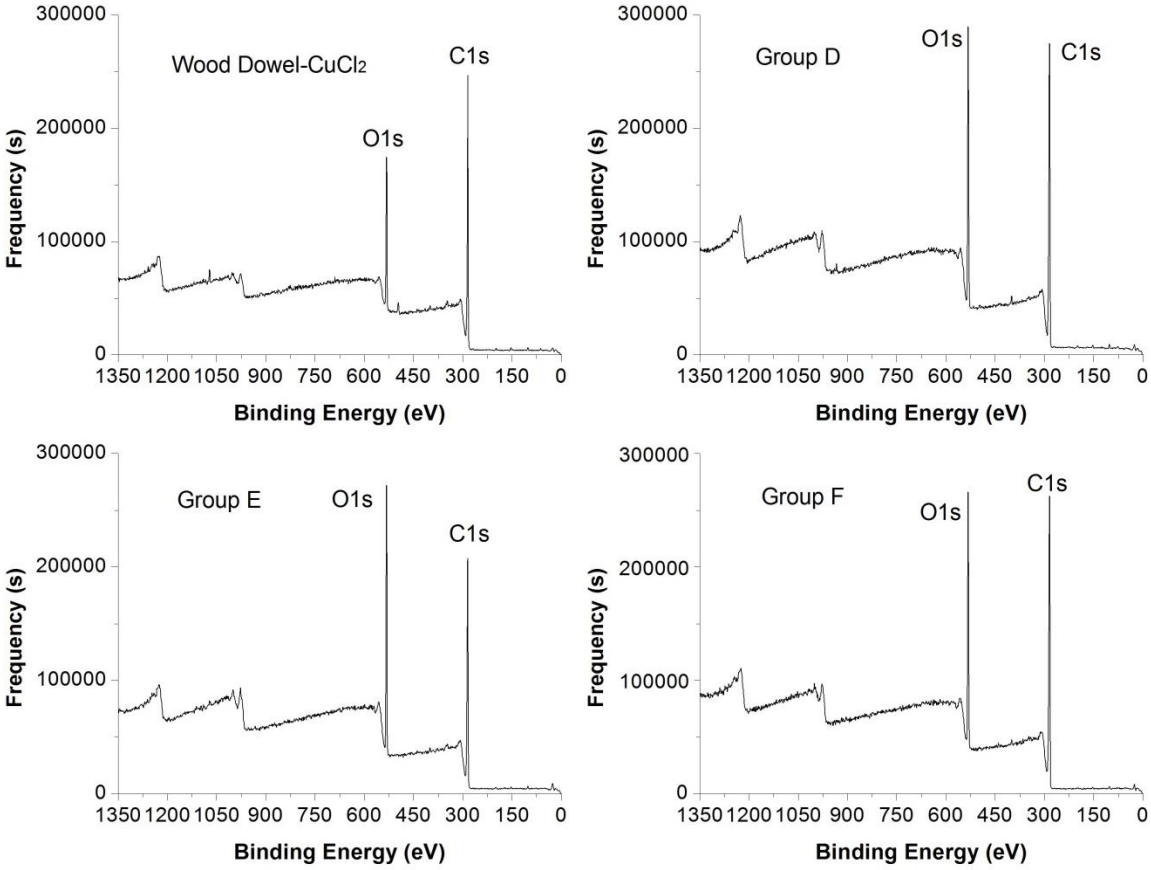

Fig. 4. XPS survey scan spectra of treated groups

The O/C ratio of the treated wood dowel was 19% higher than that of the untreated wood dowel. The acid hydrolysis of birch wood dowel in the $CuCl_2$ acid solution might be the reason for the higher ratio. From Fig. 5, the acid hydrolysis of cellulose and lignin-carbohydrate complex occurred. For cellulose, it was the long chain breaking into short chains. For lignin-carbohydrate complex, it was the cleavage of ether bonds. Hemicellulose is composed of xylan and other polysaccharides. It was acid hydrolyzed to oligosaccharide. The O/C ratios of treated groups D and E were higher than those of untreated groups A and B, respectively. This was caused by the higher O/C ratios of treated wood dowel, so then more oxygenated substance was generated in the welding interface of treated groups. However, the O/C ratio of treated group F was lower than that of untreated group C. The main explanation was that there was more molten materials and smoke-contained oxygen spilling from the welding interface of group F.

From Table 3, small amounts of elements Cu and Cl were found in the treated groups. This indicated that $CuCl_2$ was present in the surface of the treated wood dowel. According to research by Liu (2016) and Liao (2003), catalysis of $CuCl_2$ occurred during the welding process. The glass transition temperature of cellulose might decrease, which was certified by thermogravimetric analysis. Then, the highest temperatures of welding interfaces of the treated groups decreased, which was similar to the results of Table 2. Based on these, more effective and higher joint strength molten materials were generated, which resulted in the higher pullout resistance of the treated groups than that of the untreated groups in Table 1.

From Table 4, the spectral peak intensity of welding interface for treated groups among the binding energy from 286 eV to 288 eV was clearly higher than that of the treated wood dowel. The content of C2 and C3 in the treated welding interface was higher than that of the treated wood dowel, while the content of C1 was lower. With the extended welding time, the content of C1 decreased, and the relative content of C2 and C3 increased. Furthermore, the relative content of C2 increased more than that of C3. When the welding time was extended to 7 s, the content of C2 was lower than that of group E, and the content of C3 was higher than that of group E. This was caused by the oxidation of a small amount of molten materials to ketone and acid groups in the welding interface.

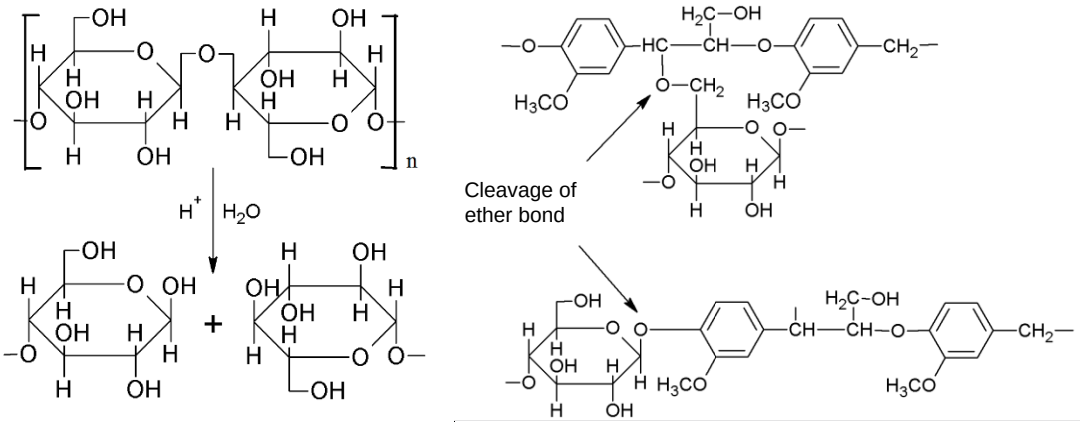

Fig. 5. Acid hydrolysis of a) cellulose and b) lignin-carbohydrate complex

According to the analysis of O1s in Table 4, the O2 content of the welding interface was higher than that of the treated wood dowel for all the treated groups. This testified that more C-O bonds was present in the welding interface. With the extended welding time, the content of O2 increased. This was caused by the generation of C-O group substance during the welding interface. However, the increase amount decreased, and the molten material and smoke that spilled from the welding interface was the reason for this.

Based on the above analysis, the enhancement mechanism of the wood dowel treated with $CuCl_2$ was that acid hydrolysis of hemicellulose and cellulose of the wood dowel occurred during immersion, which promoted the formation of molten materials by the depolymerization and pyrolysis of wood constituents. The decrease of glass transition temperature of cellulose promoted the formation of molten materials. With the same welding time, the content of oxygen-containing materials with treated samples was higher than in the untreated samples, which indicated that more pyrolysis and molten reactions occurred in the treated welding interface.

PY-GC/MS

The PY-GC/MS spectra of the untreated wood dowel, treated wood dowel, group A, and group D are shown in Fig. 6. Several differences existed between the wood dowel and welding interface, as well as the untreated groups and treated groups, especially in the area of 10 min to 20 min. According to the previous study on the pyrolysis behavior of cellulose, hemicellulose, and lignin, it was found that almost all the levoglucosan was generated from cellulose, acetic acid, and furfural from hemicellulose (Stamm *et al*. 2006; Omrani *et al*. 2008; Sun *et al*. 2010). The aromatic ring structure of lignin was stable. In contrast, some acetic acid was be generated from the branched chain of lignin. The main constituents of the samples after pyrolysis are classified in Table 5.

Table 5. Pyrolysis Main Constituents of Wood Dowel and Welding Interface

Retention Time (min)	Compound	Retention Time (min)	Compound
2.29	Acetic acid	18.14	3,5-dimethoxy-4-hydroxyphenylpropylene
4.93	Furfural	18.21	3,5-dimethoxy-4-hydroxyphenylpropylene
9.34	2-methylphenol	18.50	3-methoxy-4-hydroxyphenylpropanol
9.79	2-methoxyphenol	18.63	3-methoxy-4-hydroxyphenylpropanol
11.25	4-methyl-2-methoxyphenol	18.73	2-methoxy-4-hydroxyphenylacrolein
11.47	4-methyl-2-methoxyphenol	18.85	2,4,6-trihydroxyphenyl ketone
12.07	Catechol	18.94	3,5-dimethoxy-4-hydroxyphenylacetic acid
12.66	3-methoxy-catechol	19.39	3,4,5-trimethoxybenzyl methane
12.75	2-methoxy-4-ethylphenol	19.48	2,4,6-trimethoxybenzyl methane
13.31	3-methyl-4-hydroxyacetophenone	19.56	3,5-dimethoxy-4-hydroxyacetone
13.82	2,6-dimethoxyphenol	20.30	2,4-dimethoxybenzyl alcohol
14.02	2-methoxy-4-ethylphenol	21.02	3,5-dimethoxy-4-hydroxyphenylacrolein
14.58	3-methoxy-4-hydroxyphenylpropylene	21.14	2,4-dimethoxy phenylacrylic acid
15.09	1,2,3-trimethoxybenzene	21.27	2,4-dimethoxy phenylacrylic acid
15.18	3-methoxy-4-hydroxyphenylpropylene	22.94	3-methoxy-4-hydroxyphenylpropylene
15.31	3-methoxy-4-hydroxyphenylpropane	25.36	3-methoxy-4-hydroxybenzaldehyde
15.71	4-methoxy-3-hydroxyacetophenone	26.23	2-hydroxy-4-methoxyacetophenone
15.85	3,4-dimethoxyphenylethane	26.46	Guaiacol
16.05	3,4,5-trimethoxybenzyl methane	27.06	Catechol
16.59	3,5-dimethoxyacetophenone	28.12	3-methyl catechol
17.58	3,5-dimethoxy-4-hydroxystyrene	28.80	3-Methoxy-4-hydroxyacetophenone
17.68	2-methoxy-4-ethyl ether phenol	29.88	4-ethyl catechol
17.78	3,5-dimethoxy-4-hydroxybenzaldehyde	30.72	β-sitosterol acetate
18.02	3,5-dimethoxy-4-hydroxyphenylpropylene	31.59	4,4'-diphenylstilbene

The main constituents in the PY-GC/MS spectra were divided into two categories: carbohydrate derivatives, mainly the pyrolysis compounds of cellulose and hemicellulose, and lignin derivatives, mainly aromatic substances with benzene rings. Then, the relative contents of carbohydrate and lignin of the wood dowel and welding interface were obtained, as shown in Table 6. The highest temperature in the welding interface was 344 °C, and that was only for a short duration. The lignin was too stable to pyrolyze with the breakage of aromatic rings. With the pyrolysis of holocellulose, the relative content of lignin and derivative increased.

From Table 6, the contents of acetic acid and carbohydrate of the welding interface were lower than those of the wood dowel, which resulted in a higher content of lignin in the welding interface. This was caused by the pyrolysis of cellulose and hemicellulose during the welding process. This phenomenon was similar to the FT-IR and XPS analysis results. With the extension of welding time, the relative content of lignin increased, but slowly. It was inferred that the pyrolysis of cellulose and hemicellulose occurred during the early stage of the welding process. This was similar to the analysis results where a small decrease of relative crystallinity occurred with the extended welding time by X-ray diffraction.

Figure 6 shows the PY-GC/MS spectra of the wood dowel and welding interface. According to the analysis of the spectra, the relative contents of carbohydrate and lignin were calculated in Table 6.

Table 6. Percentages of Lignin Derivatives and Carbohydrate Released from Wood Dowel and Welding Interface for Each Group

Test Group	Carbohydrate	Lignin Derivatives	Acetic Acid
Untreated Wood Dowel	61.23	38.77	27.88
Group A	35.79	64.21	14.54
Group B	33.57	66.43	12.84
Group C	28.96	71.04	9.60
Treated Wood Dowel	51.91	48.09	13.3
Group D	44.73	55.27	12.47
Group E	40.13	59.87	12.42
Group F	39.46	60.54	10.57

Compared with the untreated wood dowel, the carbohydrate of treated wood dowel decreased clearly, while the lignin derivatives increased. This phenomenon testified that acid hydrolysis of cellulose and hemicellulose occurred during the immersion process. The relative content of lignin from the welding interface of group D was slightly higher than that of the treated wood dowel. This was caused by the pyrolysis of cellulose and hemicellulose. According to the thermogravimetric analysis, the pyrolysis degree of cellulose and hemicellulose was promoted substantially by the facilitation of $CuCl_2$. Additionally, the pyrolysis of lignin aromatic rings occurred. This result was similar to the analysis of FT-IR spectrum and the disappeared peak of 1501 cm^{-1} from the research by Liu (2016). The unit of phenylpropane structure was changed to carbonium ion (Fig. 7), and then the pyrolysis of lignin occurred. In contrast, in the presence of oxygen, the 2,3,5-thrimethylphenol was changed to quinones that could be further pyrolyzed under the promotion of $CuCl_2$. With the extension of welding time, the relative content of lignin

increased slowly. This was caused by two factors. First, it was caused by the pyrolysis of lignin as illustrated above. Second, it was caused by the molten materials spilled over the welding interface as well as the new molten materials generated with inadequate pyrolysis reaction, especially the low temperature of the bottom of the hole with little pyrolysis reaction.

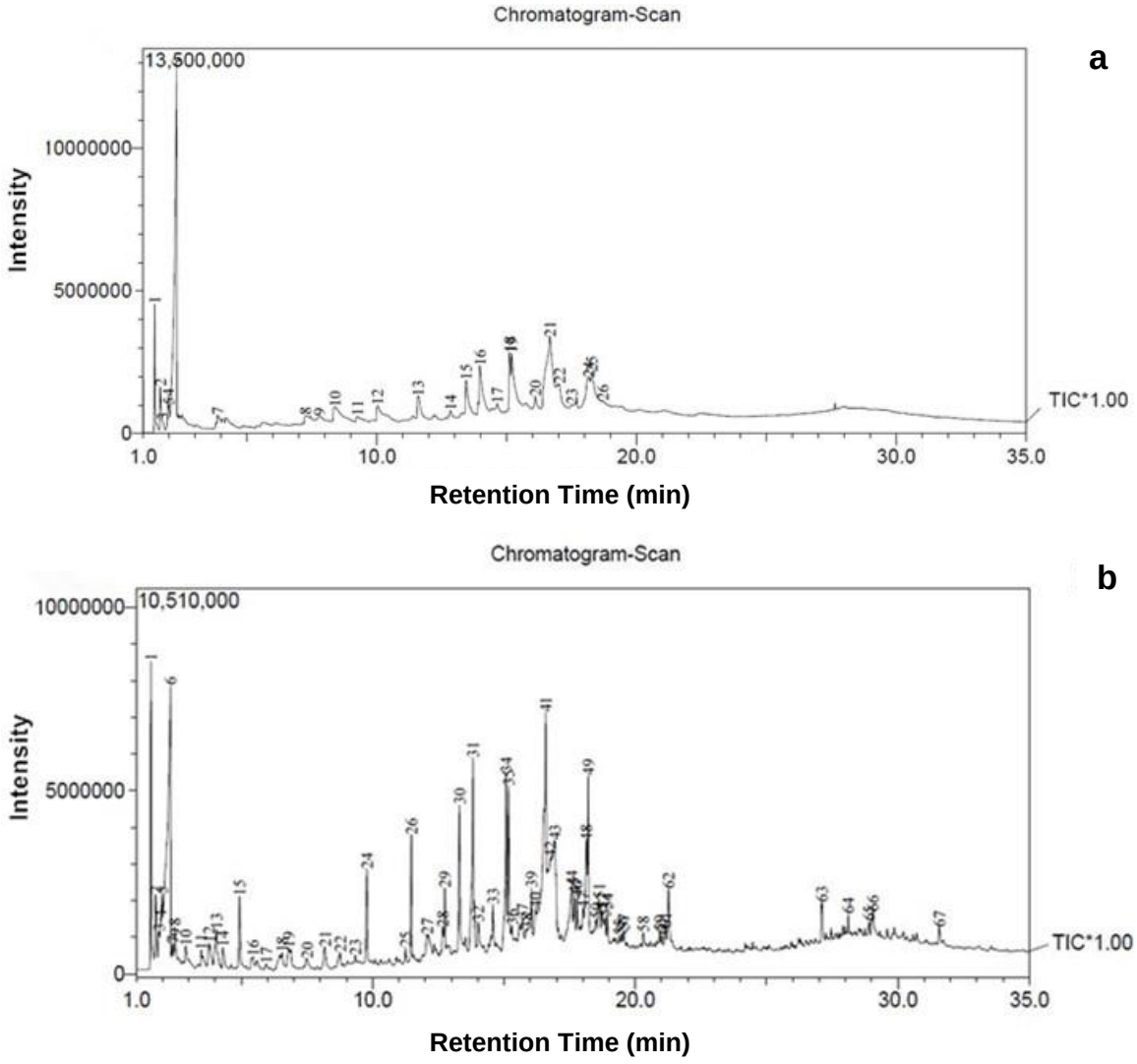

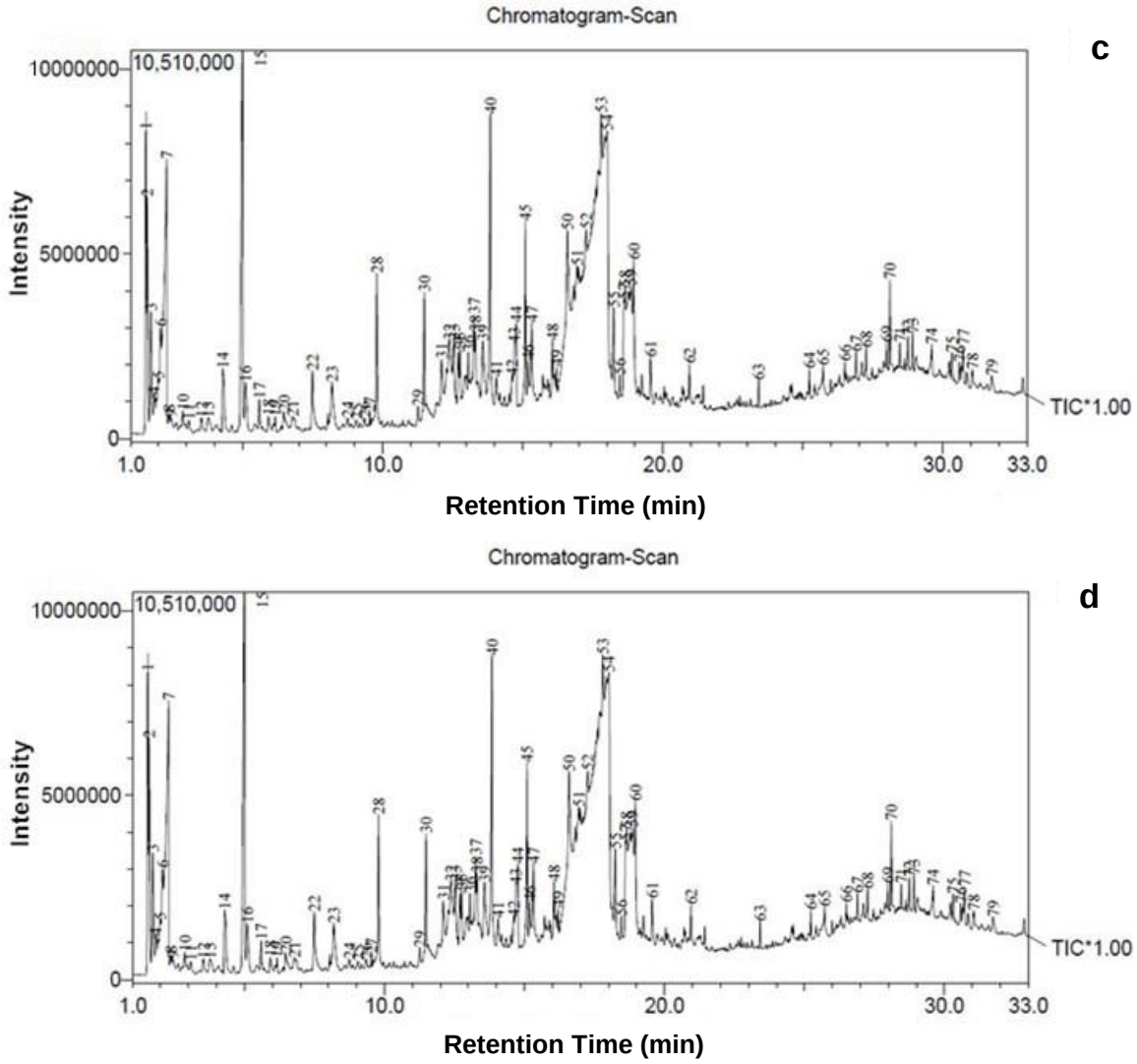

Fig. 6. PY-GC/MS spectra: a) Wood dowel; b) Welding interface of group A; c) Wood dowel pretreated with $CuCl_2$; d) Welding interface of group D

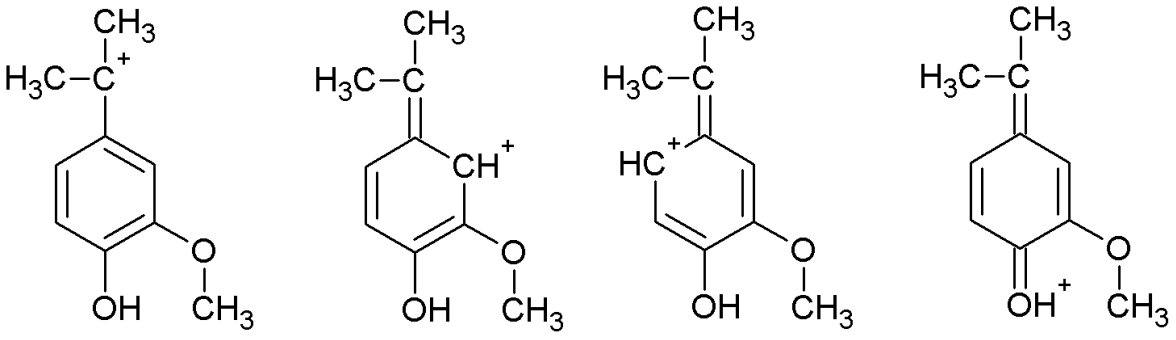

Fig. 7. Changes with lignin units in acidic medium

CONCLUSIONS

1. Rotation welding enabled the joining of wood dowels and substrates with considerable strength. The samples manufactured with the dowels immersed in $CuCl_2$ that were welded for 3 s showed the highest pullout resistance.
2. The optimal highest temperatures for untreated and treated groups with the *Betula* dowel and *Larch* substrate were 344.0 °C and 265.6 °C, respectively.
3. The mechanism of *Betula* wood dowel welded into *Larch* was that fiber was covered by the molten materials of pyrolyzed hemicellulose and amorphous materials in the welding interface during the rotation friction process. Wood constituents were pyrolyzed by the frictional heat generated from rotational welding to form oxygen-containing materials, most of which were C-O materials. With the extension of welding time, welding interface materials were pyrolyzed deeper, but the rate of pyrolysis decreased. This indicated that the pyrolysis of hemicellulose and cellulose had occurred in the prior period of the welding process.
4. The enhancement mechanism of the wood dowel treated with $CuCl_2$ was that acid hydrolysis of hemicellulose and cellulose of wood dowel might occur during immersion, which promoted the formation of molten materials by the depolymerization and pyrolysis of wood constituents. With the same welding time, the content of oxygen-containing materials with treated samples was higher than with untreated samples, which indicated that more pyrolysis and molten reactions occurred in the treated welding interface.

ACKNOWLEDGMENTS

The authors are grateful for the support of the National Natural Science Foundation of China (Grant No. 31901252), the National Natural Science Foundation of China (Grant No. 31770602), the National Key R&D Program of China (Grant No. 2017YFC 0703503), the Natural Science Foundation of Jiangsu Province, China (Grant No. BK20180276), the Natural Science Foundation of the Jiangsu Higher Education Institutions of China (Grant No. 18KJB220012), the Natural Science Foundation of the Jiangsu Higher Education Institutions of China (Grant No. 19KJD220002), and the Yangzhou Polytechnic Institute Project (Grant No. 2019xjzk007).

REFERENCES CITED

Amirou, S., Pizzi, A., Belleville, B., and Delmotte, L. (2017a). "Water resistance of natural joint of spruce produced by linear friction welding without any treatment," *International Wood Products Journal* 8(4), 201-207. DOI: 10.1080/20426445.2017.1389834

Amirou, S., Pizzi, A., and Delmotte, L. (2017b). "Citric acid as waterproofing additive in butt joints linear wood welding," *Eur. J. Wood Wood Prod.* 75(4), 651-654. DOI: 10.1007/s00107-017-1167-x

Auchet, S., Segovia, C., Mansouri, H. R., Meausoone, P.-J., Pizzi, A., and Omrani, P. (2010). "Accelerating *vs.* constant rate of insertion in wood dowel welding," *J. Adhes. Sci. Technol.* 24(7), 1319-1328. DOI: 10.1163/016942409X12598231568384

Belleville, B., Stevanovic, T., Cloutier, A., Pizzi, A., Prado, M., Erakovic, S., Diouf, P. N., and Royer, M. (2013a). "An investigation of thermochemical changes in Canadian hardwood species during wood welding," *Eur. J. Wood Wood Prod.* 71(2), 245-257. DOI: 10.1007/s00107-013-0671-x

Belleville, B., Stevanovic, T., Pizzi, A., Cloutier, A., and Blanchet, P. (2013b). "Determination of optimal wood welding parameters for two North American hardwood species," *J. Adhes. Sci. Technol.* 27(5-6), 566-576. DOI: 10.1080/01694243.2012.687596

Belleville, B., Ozarska, B., and Pizzi, A. (2016). "Assessing the potential of wood welding for Australian eucalypts and tropical species," *Eur. J. Wood Wood Prod.* 74(5), 753-757. DOI: 10.1007/s00107-016-1067-5

Belleville, B., Amirou. S., Pizzi, A., and Ozarska, B. (2017). "Optimization of wood welding parameters for Australian hardwood species," *BioResources* 12(1), 1007-1014. DOI: 10.15376/biores.12.1.1007-1014

Belleville, B., Koumba-Yoya, G., and Stevanovic, T. (2019). "Effect of wood welding process on chemical constituents of Australian eucalyptus," *J. Wood Chem. Technol.* 39(1), 43-56. DOI: 10.1080/02773813.2018.1494745

Bocquet, J.-F., Pizzi, A., Despres, A., Mansouri, H. R., Resch, L., Michel, D., and Letort, F. (2007). "Wood joints and laminated wood beams assembled by mechanically-welded wood dowels," *J. Adhes. Sci. Technol.* 21(3-4), 301-317. DOI: 10.1163/156856107780684585

Chen, M., and Lyu, J.-H. (2018). "Properties of double dowel joints constructed of medium density fiberboard," *Maderas. Ciencia y Tecnologia* 20(3), 369-380. DOI: 10.4067/S0718-221X2018005003801

Chen, M., Li, X.-M., and Lyu, J.-H. (2018). "Influence of dowel diameter and curing time on strength of double dowel joint," *Wood Research* 63(4), 591-598.

Chen, M., Li, S.-G., and Lyu, J.-H. (2019). "Effects of Selected Joint Parameters on Tensile Strength of Steel Bolt-nut Connections in *Cupressus funebris* Wood," *BioResources*. 14(3), 5188-5211.

Delmotte, L., Ganne-Chedeville, C., Leban, J. M., Pizzi, A., and Pichelin, F. (2008). "CP-MAS ^{13}C NMR and FT-IR investigation of the degradation reactions of polymer constituents in wood welding," *Polym. Degrad. Stab.* 93(2), 406-412. DOI: 10.1016/j.polymdegradstab.2007.11.020

Fukuta, S., Ogawa, K., Nomura, M., Yamasaki, M., and Sasaki, Y. (2017). "Shear properties of metal-free wooden load-bearing walls using plywood jointed with a combination of adhesive tape and wood dowels," *Eur. J. Wood Wood Prod.* 75(3), 429-437. DOI: 10.1007/s00107-016-1084-4

Kanazawa, F., Pizzi, A., Properzi, M., Delmotte, L., and Pichelin, F. (2005). "Parameters influencing wood-dowel welding by high-speed rotation," *J. Adhes. Sci. Technol.* 19(12), 1025-1038. DOI: 10.1163/156856105774382444

Korte, H., Koch, G., Krause, K. C., Koddenberg, T., and Siemers, S. (2018). "Wood nails to fix softwoods: Characterization of structural deformation and lignin modification," *Eur. J. Wood Wood Prod.* 76(3), 979-988. DOI: 10.1007/s00107-018-1288-x

Leban, J.-M., Mansouri, H. R., Omrani, P., and Pizzi, A. (2008). "Dependence of dowel welding on rotation rate," *Holz Roh. Werkst.* 66(3), 241-242. DOI: 10.1007/s00107-008-0228-6

Liao, Y. F. (2003). *Mechanism Study of Cellulose Pyrolysis*, Ph.D. Dissertation, Zhejiang University, Hangzhou, China.

Liu, Z. G. (2016). *Pore Formation Mechanism and Adsorption Property of Activated Carbon Fiber from Liquefied Wood by $ZnCl_2$*, Ph.D. Dissertation, Beijing Forestry University, Beijing, China.

Luo, X. Y., Zhu, X. D., Zhang, J. R., and Gao, Y. (2017). "Theoretical research and technical progress of wood welding," *Journal of Northwest Forestry University* 32(6), 270-275. DOI: 10.3969/j.issn.1001-7461.2017.06.43

Mougel, E., Segovia, C., Pizzi, A., and Thomas, A. (2011). "Shrink-fitting and dowel welding in mortise and tenon structural wood joints," *J. Adhes. Sci. Technol.* 25(1-3), 213-221. DOI: 10.1163/016942410X503320

O'Loinsigh, C., Oudjene, M., Shotton, E., Pizzi, A., and Fanning, P. (2012). "Mechanical behaviour and 3D stress analysis of multi-layered wooden beams made with welded-through wood dowels," *Compos. Struct.* 94(2), 313-321. DOI: 10.1016/j.compstruct.2011.08.029

Omrani, P., Masson, E., Pizzi, A., and Mansouri, H. R. (2008). "Emission of gases and degradation volatiles from polymeric wood constituents in friction welding of wood dowels," *Polym. Degrad. Stab.* 93(4), 794-799. DOI: 10.1016/j.polymdegradstab.2008.01.017

Peña, M. I. P., Deutschle, A. L., Saake, B., Pizzi, A., and Pichelin, F. (2016). "Study of the solubility and composition of welded wood material at progressive welding times" *Eur. J. Wood Wood Prod.* 74(2), 191-201. DOI: 10.1007/s00107-015-0991-0

Peña, M. I. P., Rheme, M., Pizzi, A., and Pichelin, F. (2015). "Mechanical properties of welded wood joints with natural additives," *Holztechnologie* 56(6), 5-9. DOI:

Pizzi, A., Despres, A., Mansouri, H. R., Leban, J.-M., and Rigolet, S. (2006). "Wood joints by through-dowel rotation welding: Microstructure, ^{13}C-NMR and water resistance," *J. Adhes. Sci. Technol.* 20(5), 427-436. DOI: 10.1163/156856106777144327

Pizzi, A., Leban, J.-M., Kanazawa, F., Properzi, M., and Pichelin, F. (2004). "Wood dowel bonding by high-speed rotation welding," *J. Adhes. Sci. Technol.* 18(11), 1263-1278. DOI: 10.1163/1568561041588192

Pizzi, A., Mansouri, H. R., Leban, J.-M., Delmotte, L., and Pichelin, F. (2011). "Enhancing the exterior performance of wood joined by linear and rotational welding," *J. Adhes. Sci. Technol.* 25(19), 2717-2730. DOI: 10.1163/016942411x556088

Pizzi, A., Zhou, X., Navarrete, P., Segovia, C., Mansouri, H. R., Peña, M. I. P., and Pichelin, F. (2013). "Enhancing water resistance of welded dowel wood joints by acetylated lignin," *J. Adhes. Sci. Technol.* 27(3), 252-262. DOI: 10.1080/01694243.2012.705512

Rodriguez, G., Diouf, P., Blanchet, P., and Stevanovic, T. (2010). "Wood-dowel bonding by high-speed rotation welding - Application to two Canadian hardwood species," *J. Adhes. Sci. Technol.* 24(8-10), 1423-1436. DOI: 10.1163/016942410X501025

Sandberg, D., Haller, P., and Navi, P. (2013). "Thermo-hydro and thermo-hydro-mechanical wood processing: An opportunity for future environmentally friendly

wood products," *Wood Mater. Sci. Eng.* 8(1), 64-88. DOI: 10.1080/17480272.2012.751935

Stamm, B., Windeisen, E., Natterer, J., and Wegener, G. (2006). "Chemical investigations on the thermal behaviour of wood during friction welding," *Wood Sci. Technol.* 40(7), 615-627. DOI: 10.1007/s00226-006-0097-2

Sun, Y., Royer, M., Diouf, P. N., and Stevanovic, T. (2010). "Chemical changes induced by high-speed rotation welding of wood - Application to two Canadian hardwood species," *J. Adhes. Sci. Technol.* 24(8-10), 1383-1400. DOI: 10.1163/016942410x500990

Zhang, J. R., Gao, Y., Zhang, J. N., and Zhu, X. D. (2018). "Influence of pretreated wood dowel with $CuCl_2$ on temperature distribution of wood dowel rotation welding," *J. Wood Sci.* 64, 209-219. DOI: 10.1007/s10086-017-1693-5

Zhou, X. J., Pizzi, A., and Du, G. B. (2014). "Research progress of wood welding technology (bonding without adhesive)," *China Adhes*. 23(6), 47-53.

Zhu, X. D., Xue, Y. Y., Zhang, S. J., Zhang, J., Shen, J., Yi, S. L., and Gao, Y. (2018). "Mechanics and crystallinity/thermogravimetric investigation into the influence of the welding time and $CuCl_2$ on wood dowel welding," *BioResources* 13(1), 1329-1347. DOI: 10.15376/biores.13.1.1329-1347

Zoulalian, A., and Pizzi, A. (2007). "Wood-dowel rotation welding - A heat-transfer model," *J. Adhes. Sci. Technol.* 21(2), 97-108. DOI: 10.1163/156856107780437435

Article submitted: June 24, 2019; Peer review completed: August 25, 2019; Revised version received: September 9, 2019; Accepted: September 12, 2019; Published: September 19, 2019.
DOI: 10.15376/biores.14.4.8785-8802